BULLETIN OF THE CHEMICAL SOCIETY OF JAPAN, VOL. 45, 757—764(1972)

Amino Wagging of the *tert*-Butylamine in $\tilde{A}$ Electronic State

Akiko Y. Hirakawa, Hideyuki Miyazaki, and Masamichi Tsuboi
Faculty of Pharmaceutical Sciences, The University of Tokyo, Bunkyo-ku, Tokyo

(Received August 24, 1971)

Ultraviolet absorption spectra of two isotopic *t*-butylamines, $(CH_3)_3CNH_2$ and $(CH_3)_3CND_2$, have been observed in their gaseous state in the spectral region 2000—2500 Å. There is an electronic band, whose 0—0 band peaks are observed respectively at 2351.2 and 2334.9 Å. The vibrational structure of the band, caused by the amino wagging vibration, was analyzed. On the basis of the observed energy levels, the potential function of the excited molecule along the amino wagging coordinate was determined; it is nearly harmonic with a small positive quartic term. The dependence of intensity on the vibrational quantum number and the intensity ratio of the fundamental and the hot bands indicate that the equilibrium structure of the amino group is the same as that of methylamine; the angle between the C–N axis and the HNH plane has been determined to be $51\pm4°$.

Every aliphatic amine has a strong electronic absorption band in the 2300 Å region. We have examined previously the vibrational structure of the bands of four isotopic methylamines.[1] The result indicated that the amino group has a plane structure in the lowest excited electronic state ($\tilde{A}$), while in the ground state ($\tilde{X}$) it has a pyramidal structure.[2] Along the amino wagging coordinate there are two potential minima separated by a barrier of 1688 cm^{-1} in height in the $\tilde{X}$ state,[3,4] whereas in the $\tilde{A}$ state the potential function is nearly harmonic up to tenth vibrational quantum states. The ammonia molecule is also planar in the lowest excited electronic state according to the result of an analysis[5] of the rovibronic spectrum of ND_3. In the work reported here we have examined the corresponding band of *t*-butylamine and its amino deuterated compound in an attempt to elucidate the effect of an adjacent bulky group on the amino wagging potential. As will be detailed below, the amino group of *t*-butylamine is also found to be planar in the lowest excited electronic state. It has been shown, however, the potential function along the amino wagging coordinate is appreciably different from that in methylamine.

Experimental

t-Butylamine was purchased from Tokyo Kasei Company. *t*-Butylamine-d_2 gas was obtained from deuterated *t*-butylamine hydrochloride by adding concentrated D_2O solution of NaOD. $(CH_3)_3CND_2 \cdot DCl$ was obtained by the exchange reaction of $(CH_3)_3CNH_2 \cdot HCl$ with D_2O. NaOD used was obtained by the reaction of metallic sodium with D_2O vapor at lower temperature. All the procedures for deuteration were carried out in a vacuum line.

Ultraviolet absorption measurements of these two isotopic *t*-butylamines in the 2000—2500 Å region were made by the use of a Hitachi EPS-3T spectrometer with a quartz prism. The calibration was made by the absorption lines of the γ system of nitric oxide in the region from 1955 to 2270 Å.[6] The relative position of each vibrational peak has been determined with an experimental error of about ±0.5 Å.

A gas cell with quartz windows and with 10 cm path length was used. The pressure of the gas was in the range

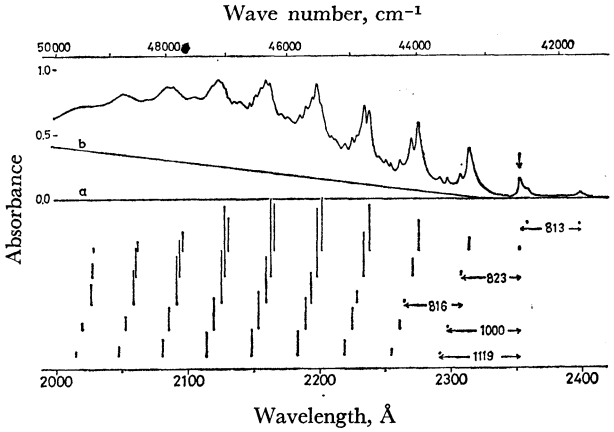

Fig. 1. The structure of the $\tilde{A}$–$\tilde{X}$ band of *t*-butylamine, $(CH_3)_3CNH_2$, in the gaseous state. The continous curve is a reproduction of the observed absorption cruve. Vertical lines indicate the calculated intensities of the bands (See the text). In the calculated spectrum the intensity ratios of the main progression ($v'_1, v'_2=v'_3=v'_4=0$) and other progressions are chosen so that it fits the observed spectrum. The arrow indicates the position of the 0—0 band. Lines a) and b) are the base lines for two possible cases (See the text).

1) M. Tsuboi, A. Y. Hirakawa, and H. Kawashima, *J. Mol. Spectrosc.*, **29**, 216 (1969).
2) T. Itoh, *J. Phys. Soc. Jap.*, **11**, 246 (1956).
3) M. Tsuboi, A. Y. Hirakawa, T. Ino, T. Sasaki, and K. Tamagake, *J. Chem. Phys.*, **41**, 2721 (1964).
4) M. Tsuboi, A. Y. Hirakawa, and K. Tamagake, *J. Mol. Spectrosc.*, **22**, 272 (1967).
5) A. E. Douglas, *Discuss. Faraday Soc.*, **35**, 158 (1963).
6) A. G. Gaydon, *Proc. Phys. Soc.*, **56**, 95 (1944).

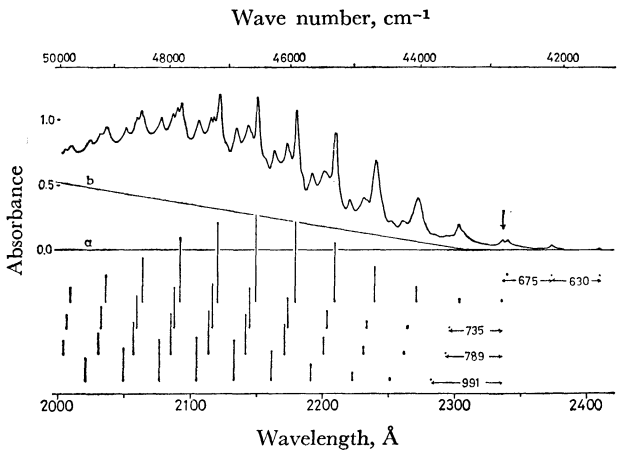

Fig. 2. The structure of the $\tilde{A}$–$\tilde{X}$ band of *t*-butylamine-d_2, $(CH_3)_3CND_2$, in the gaseous state. The continous curve is a reproduction of the observed curve. Vertical lines indicate the calculated intensities of the bands (See the text). In the calculated spectrum, the intensity ratios of the main progression (v'_1, $v'_2=v'_3=v'_4=0$) and other weak progressions are chosen so that it fits the observed spectrum. The arrow indicates the position of the 0—0 band. Lines a) and b) are the base lines for two possible cases (See the text).

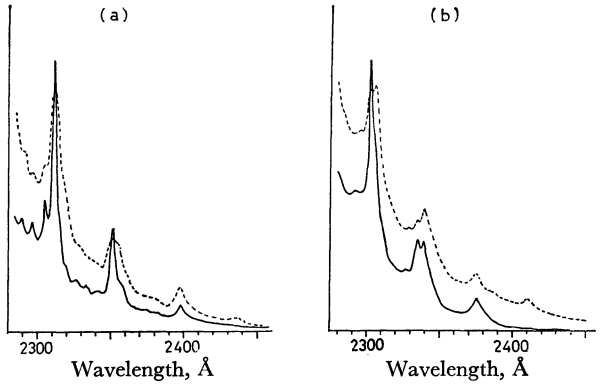

Fig. 3. Temperature dependence of the absorption intensities (a) of $(CH_3)_3CNH_2$ and (b) of $(CH_3)_3CND_2$. The solid line indicates the spectrum at 300°K and the dotted line at 350°K.

of 0.5—1.5 mmHg to obtain spectra of suitable absorption intensity. In Figs. 1 and 2, the absorption curves of two isotopic *t*-butylamine obtained at 300°K are given. To distinguish the hot bands (v'←1) from the fundamental bands (v'←0), the spectra at 350°K were also examined and are given in Fig. 3.

Experimental Results and Analysis of the Spectra

The ultraviolet absorption spectrum of *t*-butylamine in the 40000—50000 cm^{-1} region consists of a few sets of long progressions of bands. First of all, the 0–0 band of each isotopic molecule was determined. The intensities of the peaks at 2397.0 and 2356.8 Å of $(CH_3)_3CNH_2$ increase as the temperature is elevated. Therefore, these peaks are assigned to hot bands and the peak at 2351.2 Å, whose intensity decreases as the temperature is raised, is assigned to the 0–0 band of A–X electronic transition. The frequency difference between the 0–1 band (the peak at 2397.0 Å) and the 0–0 band is 813 cm^{-1}, and this agrees with the frequency of the amino wagging vibration, 811 cm^{-1} observed in the infrared absorption spectrum.[7] Similarly, for $(CH_3)_3CND_2$, the temperature effects on the spectrum show that the peaks at 2408.3, 2372.3, 2338.9, and 2306.1 Å are hot bands and the peak at 2334.9 Å is assignable to the 0–0 band. The frequency difference between the 0–1 band (the peak at 2372.3 Å) and the 0–0 band, 675 cm^{-1}, is equal to the infrared absorption frequency, 673 cm^{-1} [7] within the experimental error.

In the analysis of the bands now in question, every detail of the observed structures should be regarded to be caused by the vibrations of the molecules. The rotational structure should not appear, because even if the rotational lines form a P or R head it should be located within 15 cm^{-1} from each band center, *i.e.* at a smaller distance than the resolution (25 cm^{-1}) of the spectrometer used. For both isotopic *t*-butylamines, all the observed vibronic bands are explained in terms of four vibrational frequencies, ν'_1, ν'_2, ν'_3, and ν'_4, of the excited state and one vibrational frequency ν''_1 of the ground state. The observed frequencies of the bands with their peak heights are given in Tables 1 and 2. Every observed frequency can be assigned to one of the calculated frequencies

$$\nu_{00}+v_1'\nu_1'+v_2'\nu_2'+v_3'\nu_3'+v_4'\nu_4'+f(v_1', v_2', v_3', v_4')-v_1''\nu_1''.$$

The assignment are shown in Tables 1 and 2 in terms of a set of vibrational quantum numbers v_1', v_2', v_3', v_4', and v_1''. The values of ν_{00}, ν'_1, ν'_2, ν'_3, ν'_4, ν''_1 and $f(v_1', v_2', v_3', v_4')$ are derived as shown in the follwing paragraphs and are given in the footnotes of Tables 1 and 2. In the bands of *t*-butylamines, there are a few long progressions of v_1'. The vibrational frequencies of the members of these progressions are given by

$$\nu(v_1') = \nu_{obs}(v_1', v_2', v_3', v_4', v_1'') - \nu_{obs}(v_1'=0, v_2', v_3', v_4', v_1''). \quad (1)$$

These frequencies $\nu(v_1')$ are given in Tables 3 and 4.

The vibrational structure of the band of the undeuterated species $(CH_3)_3CNH_2$ looks slightly complicated, because there is a short progression of v_2' as well as the long progression of v_1'. In other words, there is a progression of progression. The intensities and frequencies of peaks crowded in the 2270 Å region, those in the 2235 Å region, those in the 2200 Å region, and those in the 2160 Å region are all well explained by considering such a progression of progression. The frequencies $\nu(v_1')$ of the members of this progression of progression are given in the second, third, and forth columns of Table 3. In addition, there are two progressions of weaker bands, whose frequencies $\nu(v_1')$ are given in the fifth and sixth column of Table 3. In the seventh column the frequencies $\nu(v_1')$ of the members of a hot band progression are given. The observed $\nu(v_1')$ values presented in the second, third, and fourth columns of Table 3 can be reprodced by an empirical formula.

$$\nu(v_1') = 702.5v_1' + 5.64(v_1')^2 - 1._0(v_1')(v_2'). \quad (2)$$

The $\nu(v_1')$ values calculated from Eq. (2) with $v_2'=0$ are given in the last column of Table 3. The cal-

7) H. Miyazaki, A. Y. Hirakawa, and M. Tsuboi, unpublished work.

Table 1. Observed peaks of the $\tilde{A}$–$\tilde{X}$ band of *t*-butylamine and their vibrational assignments

Å	cm^{-1}	I_h[a]	Assignment[b]					Å	cm^{-1}	I_h	Assingment				
			v_1'	v_2'	v_3'	v_4'	v_1''				v_1'	v_2'	v_3'	v_4'	v_1''
2434.9	41069	<0.001	0	0	0	0	2	2201.2	45430	0.745	4	0	0	0	0
2397.0	41718	0.040	0	0	0	0	1	2197.1	45515	0.880	3	1	0	0	0
2356.8	42430	0.067	1	0	0	0	1	2194.0	45579	0.782	2	2	0	0	0
2351.2	42531	0.145	0	0	0	0	0	2189.6	45670	0.695	3	0	1	0	0
2312.3	43247	0.375	1	0	0	0	0	2185.6	45754	0.641	3	0	0	1	0
2306.6	43354	0.182	0	1	0	0	0	2174.4	45990	0.635					
2297.2	43531	0.147	0	0	1	0	0	2169.0	46104	0.655					
2290.9	43650	0.155	0	0	0	1	0	2165.0	46189	0.750	5	0	0	0	0
2274.2	43971	0.580	2	0	0	0	0	2161.6	46262	0.890	4	1	0	0	0
2269.8	44056	0.445	1	1	0	0	0	2158.6	46326	0.905	3	2	0	0	0
(2264.0	44170	0.360)	0	2	0	0	0	2155.2	46400	0.850	4	0	1	0	0
2261.0	44228	0.295	1	0	1	0	0	2151.2	46486	0.800	4	0	0	1	0
2254.3	44359	0.275	1	0	0	1	0	2146.7	46584	0.745					
2249.6	44452	0.290						2139.3	46745	0.750					
2244.9	44546	0.318						2135.5	46828	0.750					
2237.8	44687	0.680	3	0	0	0	0	2131.2	46922	0.770	6	0	0	0	0
2233.5	44773	0.719	2	1	0	0	0	2127.2	47010	0.850	5	1	0	0	0
2229.0	44863	0.490	1	2	0	0	0	2124.0	47081	0.900	4	2	0	0	0
2224.9	44946	0.472	2	0	1	0	0	2121.3	47141	0.905	5	0	1	0	0
2219.7	45051	0.423	2	0	0	1	0	2117.7	47222	0.875	5	0	0	1	0
2212.7	45193	0.448						2086.6	47925	0.860	6	0	1	0	0
2209.0	45270	0.482						2083.4	47999	0.860	6	0	0	1	0

a) Peak height

b) Every observed frequency is nearly equal to a calculated frequency, $42531+702.5\,v_1'+5.64\,(v_1')^2+823\,v_2'+1000\,v_3'+1119\,v_4'-813\,v_1''$

Table 2. Observed peaks of the $\tilde{A}$–$\tilde{X}$ band of *t*-butylamine-d_2 and their vibrational assignments

Å	cm^{-1}	I_h[a]	Assignment[b]					Å	cm^{-1}	I_h	Assingment				
			v_1'	v_2'	v_3'	v_4'	v_1''				v_1'	v_2'	v_3'	v_4'	v_1''
2408.3	41523	0.007	0	0	0	0	2	2161.8	46258	0.761	4	0	0	1	0
2372.3	42153	0.023	0	0	0	0	1	2153.9	46427	0.720	*t*-bytyl NHD				
2338.9	42755	0.062	1	0	0	0	1	2149.1	46531	1.177	6	0	0	0	0
2334.9	42828	0.065	0	0	0	0	0	2144.9	46622	0.889	5	1	0	0	0
2306.1	43363	0.135	2	0	0	0	1	2143.2	46659	0.929	5	0	1	0	0
2302.6	43429	0.190	1	0	0	0	0	2133.3	46876	0.923	5	0	0	1	0
2295.5	43563	0.100	0	1	0	0	0	2125.9	47039	0.828	*t*-butyl NHD				
2292.7	43617	0.100	0	0	1	0	0	2120.3	47163	1.188	7	0	0	0	0
2282.1	43819	0.114	0	0	0	1	0	2116.8	47241	1.010	6	1	0	0	0
2270.7	44039	0.398	2	0	0	0	0	2114.5	47293	1.010	6	0	1	0	0
(2264.3	44164	0.207)	1	1	0	0	0	2104.7	47513	0.985	6	0	0	1	0
2261.5	44218	0.217	1	0	1	0	0	2091.8	47806	1.130	8	0	0	0	0
2251.1	44423	0.223	1	0	0	1	0	2089.2	47865	1.088	7	1	0	0	0
2239.1	44661	0.683	3	0	0	0	0	2086.7	47923	1.042	7	0	1	0	0
(2233.9	44765	0.370)	2	1	0	0	0	2076.9	48149	1.008	7	0	0	1	0
2231.2	44819	0.400	2	0	1	0	0	2063.6	48459	1.030	9	0	0	0	0
2220.2	45041	0.382	2	0	0	1	0	2062.0	48497	1.045	8	1	0	0	0
2208.5	45280	0.890	4	0	0	0	0	2059.3	48560	1.007	8	0	1	0	0
(2203.7	45378	0.555)	3	1	0	0	0	2050.0	48780	0.935	8	0	0	1	0
2201.1	45432	0.595	3	0	1	0	0	2035.2	49135	0.932	10	0	0	0	0
2190.9	45643	0.580	3	0	0	1	0	2030.9	49239	0.890	9	1	0	0	0
2183.2	45804	0.590	*t*-butyl NHD					2024.2	49402	0.840	9	0	0	1	0
2178.5	45903	1.063	5	0	0	0	0	2008.3	49793	0.790	11	0	0	0	0
(2173.8	46002	0.750)	4	1	0	0	0	2005.6	49860	0.775	10	1	0	0	0
2172.0	46041	0.810	4	0	1	0	0								

a) Peak height

b) Every observed frequency is nearly equal to a calculated frequency, $42828+601.1\,v_1'+2.70\,(v_1')^2+735\,v_2'+789\,v_3'+991\,v_4'-675\,v_1''$

Table 3. Vibrational frequencies in the long progressions of v_1' of *t*-butylamine in $\tilde{A}$ state

			obs[b]				calc[c]
v_1''(813)[a]	0	0	0	0	0	1	0
v_2'(823)	0	1	2	0	0	0	0
v_3'(1000)	0	0	0	1	0	0	0
v_4'(1119)	0	0	0	0	1	0	0
$v_1'=0$	0	0	0	0	0	0	0
1	716	702	693	697	709	712	708
2	1440	1419	1409	1415	1401		1428
3	2156	2161	2156	2139	2104		2158
4	2899	2908	2911	2869	2836		2903
5	3658	3656		3610	3572		3654
6	4391			4394	4349		4418

a) The values of v_1'', v_2', v_3', and v_4' are given in parentheses (in cm^{-1}).
b) $v(v_1')$ given by Eq. (1).
c) Calculated values by Eq. (2).

Table 4. Vbrational frequencies in the long progressions of v_1' of *t*-butylamine-d_2 in $\tilde{A}$ state (See Text)

			obs[b]			calc[c]
v_1'(675)[a]	0	0	0	0	1	0
v_2'(735)	0	1	0	0	0	0
v_3'(789)	0	0	1	0	0	0
v_4'(991)	0	0	0	1	0	0
$v_1'=0$	0	0	0	0	0	0
1	601	601	601	604	602	604
2	1211	1202	1202	1222	1211	1213
3	1833	1815	1815	1824		1828
4	2452	2439	2424	2439		2448
5	3075	3059	3042	3057		3073
6	3703	3678	3676	3694		3704
7	4335	4302	4306	4330		4340
8	4978	4934	4943	4961		4982
9	5631	5572	5622	5583		5629

a) The values v_1', v_2', v_3', and v_4' are given in parentheses (in cm^{-1}).
b) $v(v_1')$ given by Eq. (1).
c) Calculated values by Eq. (3).

culated values are in an agreement not only with the observed values of the main progression, but also with those of the two progressions of v_2' progression, because the cross term between v'_1 and v_2', ($x_{12}=-1.0$) is negligibly small. The cross terms (x_{13} and x_{14}) between v_1' and v_3' and between v_1' and v_4' are considered to be a little larger than x_{12}. They are estimated to be -7.5 and -13 respectively.

The vibrational structure of the band of the deuterated species $(CH_3)_3CND_2$ is simpler. There is a main progression whose members are markedly strong and easily picked out. Their frequencies are given in the second column of Table 4. Three other progressions of weak bands, whose frequencies are given in the third, fourth, and fifth columns of Table 4, are also easily found out. In the sixth column of Table 4, the frequencies $v(v_1')$ of the members of a hot progression are given. The observed $v(v_1')$ values of the main progression (second column of Table 4) can be reproduced by an empirical formula

$$v(v_1') = 601.1v_1' + 27.0(v_1')^2. \quad (3)$$

The $v(v_1')$ values calculated from Eq. (3) are given in the last column of Table 4. The cross terms x_{12}, x_{13}, and x_{14} are estimated to be -4.4, -4.5, and -14 respectively.

Amino Wagging Potential for the Upper State

The energy value of the vibronic levels for the upper state of the main progression is now found to be expressed in the form

$$\nu = \nu_e + \omega_1\left(v_1'+\frac{1}{2}\right) + x_{11}\left(v_1'+\frac{1}{2}\right)^2. \quad (4)$$

On the basis of the empirical formula (2) and (3), $\nu_e=41771$, $\omega_1=696.9$, and $x_{11}=5.64$ cm^{-1} for the undeuterated species and $\nu_e=42528$, $\omega_1=598.4$, and $x_{11}=2.70$ cm^{-1} for the deuterated species. The frequency appearing in the main progression (with the suffix 1) is assigned to the amino wagging vibration. This assignment is based upon its frequency (696.9 cm^{-1}), the isotope effect on its frequency (598.4 cm^{-1} for the ND_2 compound), and the character of the electronic band now in question. The band is considered to be caused by a transition in which one of the lone pair electrons on the nitrogen atom is taken up from its original orbital onto the 3*s* orbital of the nitrogen atom.[8] For such a transition, the most pronounced change in the geometrical structure of the molecule is expected

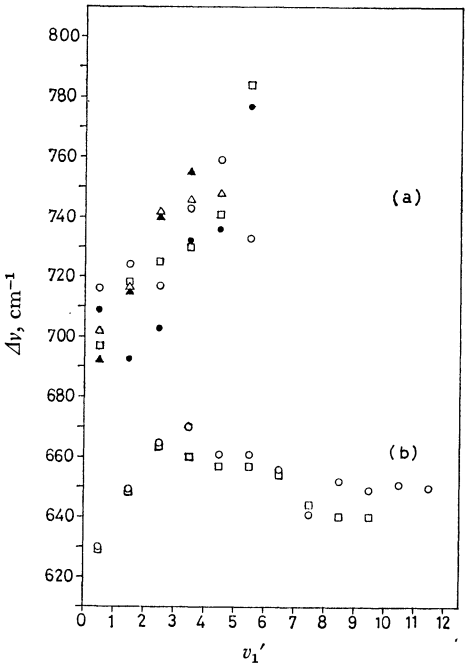

Fig. 4. Spacing of the adjacent vibronic bands in the progression of the amino wagging vibration in the $\tilde{A}$–$\tilde{X}$ band plotted against the vibrational quantum number v_1' for this vibration. (a) For $(CH_3)_3CNH_2$, ○ (for the main progression), △(for the $v_2'=1$ progression), ▲(for the $v_2'=2$ progression), □(for the $v_3'=1$ progression) and ●(for the $v_4'=1$ progression). (b) For CH_3NH_2, ○(for the main progression) and □(for the $v_2'=1$ progression).

8) K. S. Mulliken, *J. Chem. Phys.*, **3**, 506 (1935).

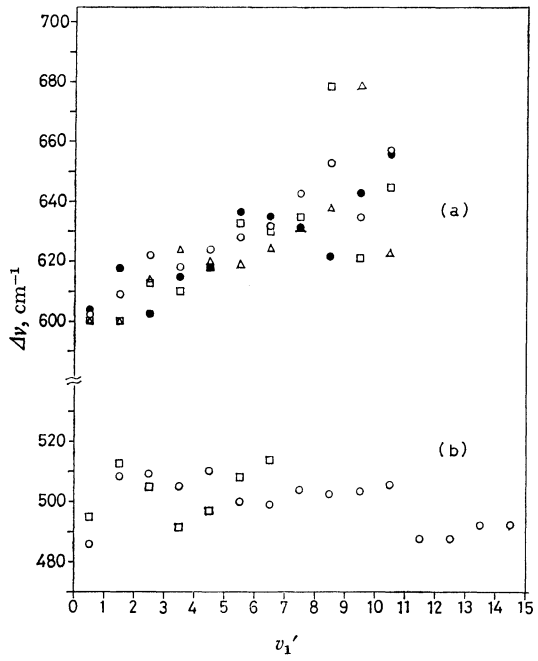

Fig. 5. Similar plotting to that in Fig. 4 for (a) $(CH_3)_3CND_2$ and (b) CH_3ND_2. For (a), ○(for the main progression), △(for the $v_2'=1$ progression), □(for the $v_3'=1$ progression) and ●(for the $v'_4=1$ progression). For (b), ○(for the main progression) and □(for the $v_2'=1$ progression).

to take place along the amino wagging coordinate, as in the case of methylamine.[1] Therefore, the amino wagging vibration is expected to form the main progression in the vibrational structure of the band. Thus, Eq. (4) is regarded to give the energy levels of the amino wagging vibration of the *t*-butylamine molecule in the $\tilde{A}$ electronic state. It is noteworthy that the interval of the adjacent levels increases with increasing v_1'. In this respect, *t*-butylamine is similar to ammonia,[9] but it presents a contrast to methylamine, for which the interval is almost independent of v_1'. This contrast is demonstrated in Figs. 4 and 5. This fact indicates that the potential function along the amino wagging coordinate involves a positive quartic term for *t*-butylamine, whereas the function is nearly harmonic for methylamine.[1]

Let us now assume that the potential function along the amino wagging coordinate, θ (the external angle between the HNH plane and the C–N bond), has the form,

$$hcV = \frac{1}{2}k\theta^2 + j\theta^4. \tag{5}$$

The potential constant k and j are related to the observed ω_1 and x_{11} as

$$\omega_1 = \frac{1}{2\pi c}\sqrt{\frac{k}{\mu}} \tag{6}$$

and

$$x_{11} = \frac{3h^2}{32\pi^4\omega_1^2\mu^2c^2}\frac{j}{hc} \tag{7}$$

where μ is the reduced moment of inertia (amu·Å^2), h the Planck's constant, and c the light velocity. A transformation, leads to the potential function,

$$Q = \sqrt{\mu}\theta, \quad (\text{in amu}^{1/2}\text{Å}) \tag{8}$$

leads to the potential function,

$$hcV = \frac{1}{2}KQ^2 + JQ^4, \tag{9}$$

where

$$K = k/\mu^2 \tag{10}$$

and

$$J = j/\mu^2. \tag{11}$$

By the use of the observed values of ω_1 and x_{11}, we obtain the potential functions,

$$V(\text{cm}^{-1}) = 7200Q^2 + 1610Q^4 \quad \text{for } (CH_3)_3CNH_2 \tag{12}$$

and

$$V(\text{cm}^{-1}) = 5310Q^2 + 567Q^4 \quad \text{for } (CH_3)_3CND_2. \tag{13}$$

The potential fuction for the excited state of *t*-butylamine -d_2 is shown graphically in Fig. 6 (a).

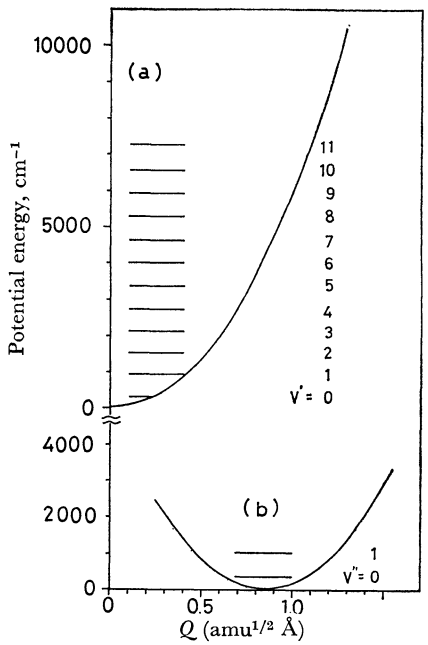

Fig. 6. Potential functions and vibrational energy levels of the amino wagging vibration of *t*-butylamine-d_2. (a) in the first excited electronic state $\tilde{A}$ and (b) in the ground state $\tilde{X}$.

Position of the Potential Minimum in the Lower State

The amino-wagging potential just described indicates that the *t*-butylamine molecule in the upper state has a planar amino group in its equilibrium conformation. It is probable, on the other hand, the amino group of *t*-butylamine is pyramidal in its ground electronic state as it is usually so in any aliphatic primary amine. In other words, the potential minimum in the lower state is considered to be greatly shifted along the amino wagging coordinate from that in the upper state as is shown in Fig. 6. The amount of shift (or the position of the potential minimum in the ground state, $Q_{\min}$) can be estimated from the intensity distribution among the members of each of the progressions mentioned above.

Thus, according to the Franck-Condon principle, the

9) A. D. Walsh and P. A. Wasrop, *Trans. Faraday Soc.*, **57**, 345 (1961).

integrated intensity I of each vibronic band $v' \leftarrow v''$ is given by

$$I = \int \varepsilon(\nu) d\nu = (8\pi^2 N \nu_{v' \leftarrow v''}/3hc) |R_e|^2 |S_{v'v''}|^2, \quad (14)$$

where N is the population in the lower state, R_e is the electronic transition moment of the band in question, and $S_{v',v''}$ is the overlap integral,

$$S_{v'v''} = \langle \phi_{v'}(Q) \cdot \phi_{v''}(Q) \rangle, \quad (15)$$

in which $\phi_{v'}$, (Q) and $\phi_{v''}(Q)$ are the vibrational eigenfunctions of the upper and lower states, respectively. In an approximation, both of these vibrational eigenfunctions are assumed to be those of harmonic oscillators, so that

$$\phi_{v'}(Q) = N_{v'} \exp[-(\gamma'/2)Q^2] H_{v'}(\sqrt{\gamma'} Q) \quad (16)$$

and

$$\phi_{v''}(Q) = N_{v''} \exp[-(\gamma''/2)(Q-Q_{\min})^2] \times H_{v''}[\sqrt{\gamma''}(Q-Q_{\min})]. \quad (17)$$

Here, $N_{v'}$ and $N_{v''}$ are the normalization factors, $\gamma' = 4\pi^2\omega'/h$, and $\gamma'' = 4\pi^2\omega''/h$. ω' and ω'' are the harmonic frequencies of the amino wagging vibrations in the upper and lower states respectively. In Eq. (14), all the fraction except $|S_{v'v''}|^2$ in the expression of the integrated intenisty are considered to be practically independent of v'. We therefore calculated $|S_{v'v''}|^2$ as a function of v' by the use of various assumed values of $Q_{\min}$, and compared the results with the observed intensities.

The relative value of absorbance determined at the peak of each vibronic band is given in Tables 1 and 2. In determining the intensities of the bands from these values a possibility of the superposition of the absorptions caused by the second electronic transition $\tilde{B} \leftarrow \tilde{X}$ must be taken into account. In each of Figs. 1 and 2, is shown by a line (b) what is considered to be the upper limit of such background absorption. In other words, the background absorption is considered to be some where between the lines (a) and (b) in Fig. 1 or 2. By subtracting this background absorption from the observed peak height, we can estimate the peak intensity of each band. The integrated intensity is considered to be proportional to the square of the peak intensity because each vibrational band should have the similar rotational structure, therefore, it has a similar contour to another.

The integrated intensities of the members of the v_1'-progressions, thus estimated, are given in Figs. 7 and 8. Each vertical line indicates a range of ambiguity caused by the difficulty of estimating the background absorption, and each range given by the line coresponds to the range (a) to (b) of the background absorption (Figs. 1 and 2).

In Figs. 7 and 8, are also shown the calculated intensities, *i.e.* the calculated values of $|S_{v'v''}|^2$ for a few different assumed values of $Q_{\min}$. The calculations were made by the use of a HITAC 5020E computer in the Computer Centre of the University of Tokyo. A comparison of the observed and calculated intensities indicates that $Q_{\min}=0.65\pm0.05$ amu$^{1/2}$ Å for $(CH_3)_3CNH_2$ and $Q_{\min}=0.85\pm0.05$ amu$^{1/2}$ Å for $(CH_3)_3CND_2$.

An estimation of the $Q_{\min}$ value can also be made

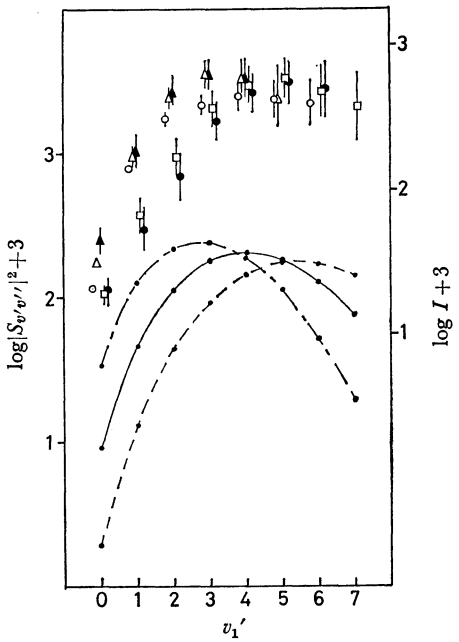

Fig. 7. The relative intensities of the vibronic bands in the progression of the amino wagging vibration of $(CH_3)_3CNH_2$, plotted against the vibrational quantum number v_1'. The points connected with curves represent the calculated values for $Q_{\min}=0.75$ amu$^{1/2}$ Å (---), for $Q_{\min}=0.65$ amu$^{1/2}$ Å (—) and for $Q_{\min}=0.55$ amu$^{1/2}$ Å (—·—·). The observed integrated intensities are shown by ○(for the main progression), △(for the $v_2'=1$ progression), ▲(for the $v_2'=2$ progression), □(for the $v_3'=1$ progression) and ●(for the $v_4'=1$ progression). The vertical line indicates the range of ambiguity of the observed intensity, which corresponds to the range of the background absorption defined by (a) and (b) in Fig. 1.

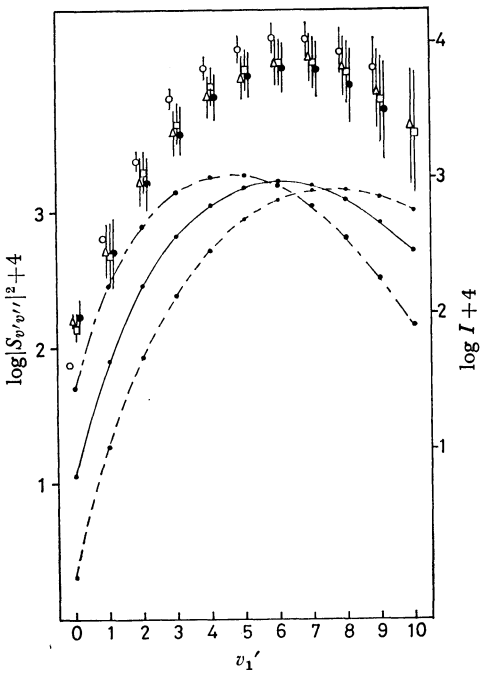

Fig. 8. Similar plotting to that in Fig. 7 for $(CH_3)_3CND_2$. The calculated values for $Q_{\min}=0.95$ amu$^{1/2}$ Å (···), for $Q_{\min}=0.85$ amu$^{1/2}$ Å (—) and for $Q_{\min}=0.75$ amu$^{1/2}$ Å (—·—·) are shown. The observed integrated intensities are shown by ○(for the main progression), △(for the $v_2'=1$ progression), □(for the $v_3'=1$ progression), and ●(for the $v_4'=1$ progression).

from the observed integrated intensity ratio (R) of the $(v'=1)\leftarrow(v''=1)$ band *versus* $(v'=0)\leftarrow(v''=0)$ band or of the $(v'=2)\leftarrow(v''=1)$ band *versus* $(v'=1)\leftarrow(v''=0)$ band. In general, a pair of bands $(v'+1)\leftarrow 1$ and $(v')\leftarrow 0$ come close to each other, and therefore in estimating the intensity ratio (R) of these bands the ambiguity caused by the background absorption is relatively small. On the other hand, the intensity ratio R should be sensitive to the Q_{min} value. A calculation has been made of the theoretical values of R for a few assumed values of Q_{min} by the use of Eqs. (15), (16), and (17). In Figs. 9 and 10, the observed and calculated intensity ratios (R) of such pairs of bands are given. In comparison, it is shown again that $Q_{min}=0.65$ amu$^{1/2}$ Å for $(CH_3)_3CNH_2$ and $Q_{min}=0.85$ amu$^{1/2}$Å for $(CH_3)_3CND_2$.

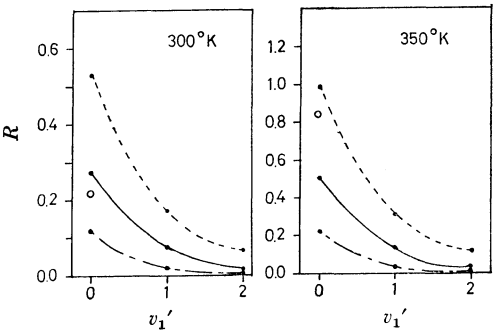

Fig. 9. Intensity ratio of the $v_1'\leftarrow 0$ band *versus* $v_1'+1\leftarrow 1$ band of *t*-butylamine plotted against v_1' at 300 and 350°K. The points connected with curves represent the calculated values for $Q_{min}=0.75$ amu$^{1/2}$ Å (---), for $Q_{min}=0.65$ amu$^{1/2}$ Å (—), and for $Q_{min}=0.55$ amu$^{1/2}$ Å (—·—·). Circles represent the observed values.

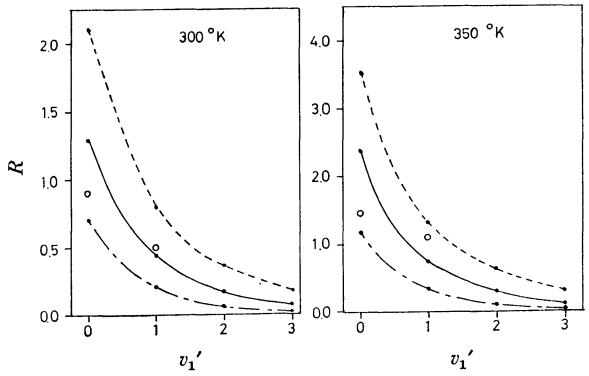

Fig. 10. Intensity ratio of the $v_1'\leftarrow 0$ band *versus* $v_1'+1\leftarrow 1$ band of *t*-butylamine-d_2 plotted against v_1' at 300 and 350°K. The points, connected with curves, represent the calculated values for $Q_{min}=0.95$ amu$^{1/2}$ Å (---), for $Q_{min}=0.85$ amu$^{1/2}$ Å (—) and for $Q_{min}=0.75$ amu$^{1/2}$ Å (—·—·). Circles represent the observed values.

Discussion

From our analysis of the bands, an amount of information has now been obtained on the potential function along the amino wagging coordinates of upper and lower states of *t*-butylamine and *t*-butylamine-d_2. The values of potential constants obtained are given in Table 5.

The position of potential minimum in the ground state has been estimated to be at $Q=0.65\pm0.05$ and 0.85 ± 0.05 amu$^{1/2}$ Å respectively for $(CH_3)_3CNH_2$ and $(CH_3)_3CND_2$. These values are equal to the corresponding values (0.655 and 0.845 amu$^{1/2}$ Å, respectively) of methylamine.[4] If we know the reduced moment of inertia μ we can estimate the equilibrium angle θ by Eq. (8). Let us assume that the value of μ is equal to the inverse of the diagonal element of the G matrix (inverse kinetic energy matrix) corresponding to the wagging coordinate of the planar amino group. Then $\mu=0.540$ amu Å^2 for $(CH_3)_3CNH_2$ and $\mu=0.885$ amu Å^2 for $(CH_3)_3CND_2$. With these values of μ, the equilibrium θ value should be $50.7\pm4°$ for $(CH_3)_3CNH_2$ and $51.7\pm3°$ for $(CH_3)_3CND_2$. Both of these are practically equal to the known value of θ (=51.3°) of methylamine.[2] Thus, the equilibrium conformation of the amino group for *t*-butylamine in the ground state is now found to be quite similar to that for methylamine.

Table 5. Estimated potential constants of amino wagging motion for *t*-butylamine and *t*-butylamine-d_2 in $\tilde{X}$ and $\tilde{A}$ electronic state

$(CH_3)_3CNH_2$		
	ground ($\tilde{X}$)	excited($\tilde{A}$)
ν_1(cm^{-1})	813	702.$_5$
ω_1(cm^{-1})	—	696.$_9$
x_{11}(cm^{-1})	—	5.6_4
Q_{min}(amu$^{1/2}$Å)	0.65±0.05	0
θ(degree)	50.$_7$°±4°	0
$(CH_3)_3CND_2$		
	ground ($\tilde{X}$)	excited ($\tilde{A}$)
ν_1(cm^{-1})	675	601.$_1$
ω_1(cm^{-1})	—	598.$_4$
x_{11}(cm^{-1})	—	2.7_0
Q_{min}(amu$^{1/2}$Å)	0.85±0.05	0
θ(degree)	51.$_7$°±3°	0

The potential function in the upper state for *t*-butylamine, on the other hand, has been found to be somewhat different from that for methylamine. As has been demonstrated in Figs. 4 and 5, the potential function is nearly harmonic in methylamine, while in *t*-butylamine the potential rises up more steeply as the wagging angle of the amino group increases. As a possible cause of the difference it may be proposed to consider the repulsive force between the bulky *t*-butyl group and the amino group. To test this proposal, a calculation of the repulsive potential has been made for various positions (θ) of the amino group in both of these amines on the basis of a probable set of bond lengths and bond angles and on the basis of potential functions for the non-bonded C···H and H···H atom pairs given by Hendrickson[10] or those given by Bartell.[11] The result indicated that at least a part of the observed difference is explained by the extra repulsive potential caused by the bulkiness of the *t*-butyl group.

Lastly, a brief discussion will be made of the observed vibrational frequencies of the undeuterated and deu-

10) J. B. Hendrickson, *J. Chem. Soc.*, **83**, 4537 (1961).
11) L. S. Bartell, *J. Chem. Phys.*, **32**, 827 (1960).

terated *t*-butylamines in the excited states. The frequency 1000 cm^{-1} of the former is considered to correspond to the frequency 991 cm^{-1} of the latter, and 1119 cm^{-1} to 789 cm^{-1}. The two frequencies 697 and 823 cm^{-1} of the undeuterated species are considered to be caused by a strong vibrational coupling. The intrinsic amino wagging frequency of the undeuterated species should be 765 cm^{-1} if it is 598 cm^{-1} in the deuterated compound. This vibration may couple with the 735 cm^{-1} vibration and may split into the 697 and 823 cm^{-1} vibrations. It is probable that the 735 cm^{-1} vibration which takes place in both deuterated and undeuterated molecules is a skeletal stretching vibration on the basis of a normal vibration calculation of isobutane[12] and of a comparison with the frequencies of *t*-butylfluoride (750 cm^{-1}),[13] *t*-butylalcohol (748 cm^{-1}) and *t*-butylalcohol-d (744 cm^{-1}).[14]

12) H. Takahashi, *Nippon Kagaku Zasshi*, **83**, 799 (1962).
13) D. E. Mann, N. Acquista, and D. R. Lide, Jr., *J. Mol. Spectrosc.*, **2**, 575 (1958).
14) C. Tanaka, *Nippon Kagaku Zasshi*, **81**, 1042 (1960).